JOURNAL OF MATERIALS SCIENCE **38** (2003) 2953–2961

Solid state reactions of cordierite precursor oxides and effect of CaO doping on the thermal expansion behaviour of cordierite honeycomb structures

R. JOHNSON, I. GANESH, B. P. SAHA, G. V. NARASIMHA RAO, Y. R. MAHAJAN*
Ceramic Materials Division, International Advanced Research Centre for Powder Metallurgy and New Materials (ARCI), Balapur PO, Hyderabad-500 005, India
E-mail: arcint@hd1.vsnl.net.in

The extruded cordierite honeycomb structure from a stoichiometric formulation of talc, kaolinite, and alumina was subjected to TGA-DSC, dilatometric and XRD investigations. The experimental observations were made to identify the phase transformation sequence in order to understand the solid state reactions involved in the cordierite formation. A maximum cordierite content of 90% was achieved for the samples sintered at 1693 K with a soaking time of 4 h, corresponding to a lowest coefficient of thermal expansion (CTE) of 0.74×10^{-6}/K (along the direction of extrusion) was observed. Attempts were made to establish correlations with cordierite content, processing temperature and CTE of the samples. A few mechanisms are proposed to explain our observations. Attempts are also made to rationalize the low CTE observed along the direction of extrusion on the basis of orientation of anisotropic cordierite crystals as revealed by the transverse I-ratio calculated from the XRD patterns. Effect of CaO doping on CTE of cordierite has been studied in the present work. It was observed that though there is an increase in bulk thermal expansion of cordierite honeycombs on CaO doping due to the absence of micro-cracks as reveled by thermal cycling hysteresis, axial anisotropy was found to be reduced significantly.

1. Introduction

Cordierite ($2MgO{\cdot}2Al_2O_3{\cdot}5SiO_2$) based honeycomb structure has received a great deal of interest because of its unique properties such as low coefficient of thermal expansion (CTE) and high thermal shock resistance [1–3]. Because of these properties, cordierite honeycombs have been extensively used for various applications such as substrates for emission control catalysts in automobiles and stationary sources [4–8], diesel particulate wall flow filters [4], ceramic gas turbine heat exchangers [9], hot gas filters [9], molten metal filters [10], etc. In the year of 2001, over 80 million cordierite substrates were used to meet the world market, making it one of the most significant technical ceramic products [4].

As naturally occurring cordierite mineral is very scarce, and impure in nature, cordierite products are obtained by following synthetic route [11]. Although cordierite products are synthesized by a number of methods such as, sol-gel [12, 13], spray pyrolysis [14] and co-precipitation [15], the most popular technique available is the solid-state reaction of precursor oxides [1, 3, 6, 16, 17] namely talc, kaolinite and alumina on account of its cost effectiveness and their abundance in combination with the adaptability for forming and firing process [18, 19]. However, these raw materials being mineral origin, the whole series of reactions involved in the cordierite formation is governed especially by the habitat, chemical composition, particle size and morphology, hence, the prior designing of the appropriate precursor oxide mix, sintering schedule and understanding of the evolution of cordierite throughout processing temperature range are very important for the optimization of the processing parameters for a particular set of raw materials. One of the most difficult problems associated with the preparation of cordierite ceramics is the narrow temperature interval for sintering which is located just below the incongruent melting point of pure cordierite [16]. This narrow temperature range demands reasonably well-controlled temperature conditions during densification. Moreover, the densification behaviour and melting point of cordierite is a direct consequence of impurities present in the precursor materials [3, 20] such as, K_2O, CaO, Fe_2O_3, etc.,

*Author to whom all correspondence should be addressed.

which significantly increases the thermal expansion coefficient of cordierite. Since, naturally occurring raw materials are associated with various impurities, it becomes necessary to understand the effect of these impurities on the key properties of honeycombs.

In the present study, a systematic work was undertaken to understand the evolution of cordierite from a set of raw materials such as talc, kaolinite and alumina. In this connection, green honeycomb extruded from talc, kaolinite and alumina in the cordierite stoichiometry was subjected to simultaneous thermogravimetry-differential scanning calorimetry (TG-DSC), dilatometric, and X-ray diffraction (XRD) studies. Further, the effect of CaO, a common impurity generally present in the talc playing a dominant role on critical properties of honeycomb has also been studied by doping the known quantities of CaO in the cordierite stoichiometry. Moreover, in order to understand the effect of configuration on thermal expansion behavior, a cylindrical solid rod was extruded and sintered. These samples were further subjected to dilatometric and XRD measurements under identical conditions.

2. Experimental

2.1. Extrusion of cordierite precursor oxides

Based on ternary phase diagram SiO_2-MgO-Al_2O_3, the specially selected raw materials such as talc, kaolinite and alumina were formulated to achieve the cordierite stoichiometry, having composition of 51 mass% SiO_2, 35 mass% Al_2O_3 and 14 mass% MgO [16]. The chemical composition and physical properties of talc, kaolinite and alumina used in this investigation are given in the Table I. Initially, a homogeneous mixture of raw materials was kneaded into extrudable dough with the addition of proper amounts of binder (methylcellulose), plasticizer (polyethylene glycol) and water in a sigma kneader. Thus obtained dough was then extruded into honeycomb structures having 100 mm diameter and 150 mm length with a channel wall thickness of 0.2 mm using an indigenously designed and fabricated extrusion die [6, 16, 17]. A part of the dough was also extruded into a cylindrical solid rod. The extrudates were dried in an oven prior to sintering in a programmable electrical furnace at heating rate of 120 K per hour up to the peak temperature of 1693 K for a soaking period of 4 h and maintaining cooling rate of 200 K per hour to room temperature. Further, cordierite raw mix was doped with 0.5 mass%, 1.0 mass% and 1.5 mass% of CaO by mass and the honeycombs were extruded and sintered under identical conditions as elaborated above.

TABLE I Physico-chemical properties of raw materials

Physico-Chemical properties	Talc	Kaolinite	Alumina
Chemical composition			
SiO_2 (mass%)	60.0	44.0	0.1
Al_2O_3 (mass%)	2.1	40.2	97.7
Fe_2O_3 (mass%)	0.6	0.4	0.2
TiO_2 (mass%)	0.08	0.4	0.18
CaO (mass%)	0.4	<0.1	0.7
MgO (mass%)	31.1	<0.1	0.1
Na_2O (mass%)	<0.01	0.11	0.33
K_2O (mass%)	<0.01	<0.01	<0.1
Moisture (%)	–	1.0	–
LOI (RT to 1273 K)	5.5	13.8	0.6
Average particle size, (μm)	21.62	2.86	6.61
BET surface area ($m^2\ g^{-1}$)	0.697	17.15	0.073
Crystalline phase	Talc	Kaolinite	α-Al_2O_3

2.2. Characterization of samples

Sintered cordierite specimens were characterized for their bulk density, apparent porosity and water absorption by Archimedes principle. In order to study, the extent of physico-chemical changes occurring in green honeycombs over the processing temperature ranges, the specimens were subjected to the simultaneous thermo-gravimetric (TGA) and differential scanning calorimetric (DSC) analysis using Netzsch, TGA-DSC-PG/PC analyzer from room temperature to 1693 K. The specimens were subjected to dilatometric analysis along as well as across the channels (i.e., direction of extrusion) using a push rod type dilatometer (Netzsch 402C) incorporating the sample holder correction to determine the linear changes taking place in the samples and hence to achieve the firing profiles.

The evolved phases corresponding to the transformations and thermal events were identified by taking very thin layers of powder samples on zero background plates, using Bruker's D8 advance XRD system with Cu-Kα radiation. The thin layer sample reduced the absorption effects taking place within the sample as most of the phases are made of low atomic number elements, hence, have greater depth of penetration and could give raise to wider Bragg peaks. The purpose of using zero background plate was to further ensure that the sample characteristic amorphous content must be made to exhibit its nature in the XRD pattern clearly, visible and should not be merged with that of the amorphous nature of the sample holder plates such as glass, plastic, perspex, etc., if used. Further, the cordierite samples doped with CaO were also subjected to dilatometric and XRD measurements and the lattice parameters were calculated.

In order to determine the thermal expansion behavior of solid rod and honeycomb, and to estimate the extent of orientation of the cordierite crystals and their effect on critical properties, XRD patterns and dilatometric curves for honeycombs (parallel and perpendicular to the channels) were recorded. Further, the transverse I ratio of the samples were calculated from the XRD data using the following Equation [3]

$$\text{Transverse } I \text{ ratio, } (I) = \frac{I_{(110)}}{I_{(110)} + I_{(002)}}$$

(where $I_{(110)}$ and $I_{(002)}$ are the heights of Bragg peaks corresponding to the cordierite (110) and (002) Miller planes).

3. Results and discussions

3.1. Thermogravimetry and differential scanning calorimetry

TG-DSC curves recorded on the green honeycomb from room temperature to 1693 K are shown in Fig. 1. As can be seen from Fig. 1, TG curve shows an initial

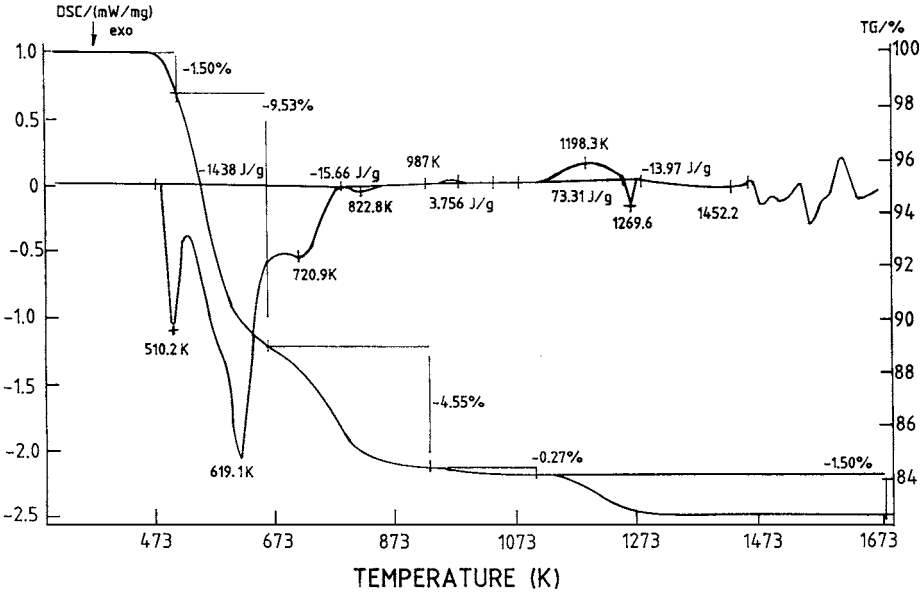

Figure 1 TG-DSC profile of honeycomb made from talc, kaolinite and alumina oven dried for overnight.

weight loss of about 1.5% between 503 and 513 K followed by a major weight change of about 9.53% in the temperature range of 553 to 623 K, which can be attributed to the pyrolytic degradation of methyl cellulose and polyethylene glycol used as binder and plasticizer, respectively, used in the extrusion of honeycomb structures [21]. Presence of exothermic DSC peaks at 510 K and 619 K with enthalpy change of 1435 J/gm further supports this observation. Another weight change of 4.55% along with an exothermic peak at 721 K and 823 K observed could be attributed to the organic burn out overlapped by the thermally induced de-hydroxylation of kaolinite [$2Al_2(OH)_4(Si_2O_5)$] to metakaolin [$2Al_2Si_2O_7$] [22]. An exothermic peak observed at 987 K may probably be due to the decomposition of minor impurities such as carbonates at these temperature ranges. Fig. 1 also shows another exothermic DSC peak and the thermo-gravimetric weight change of 1.5% in the temperature range of 1173 K to 1223 K. This may probably be due to the removal of structural water resulting from the dehydroxilation at these temperature ranges. After this transformation, there appears to be no major thermo-gravimetric weight change occurring up to 1693 K, however, many exothermic and endothermic DSC peaks are observed in the temperature range of 1473 K to 1673 K due to solid state reactions of decomposition products leading to the formation of cordierite. These results are in good agreement with the previous studies [23].

3.2. Thermo-dilatometric studies

Dilatometric curve of the green honeycombs recorded from room temperature to 1693 K is shown in Fig. 2. As can be seen from Fig. 2, that a linear shrinkage of 0.13% at 773 to 823 K and 0.86% in the temperature range of 1173 to 1223 K coincides with the transitions observed in TG-DSC curves as explained above (Fig. 1). A major slope change in the temperature range of 1423 K to 1523 K can be attributed to the transformation of amorphous

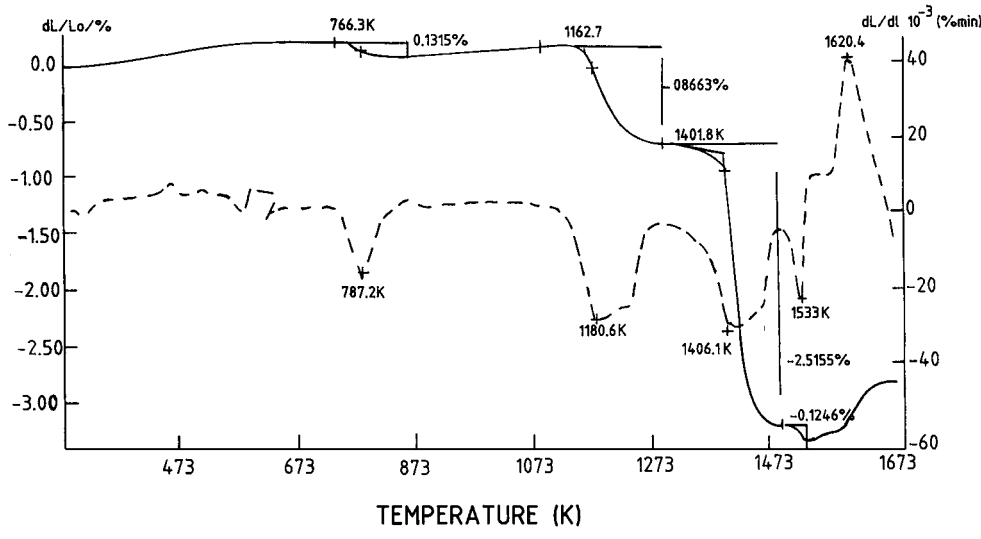

Figure 2 Dilatometry profile of honeycomb made from talc, kaolinite and alumina oven dried for overnight.

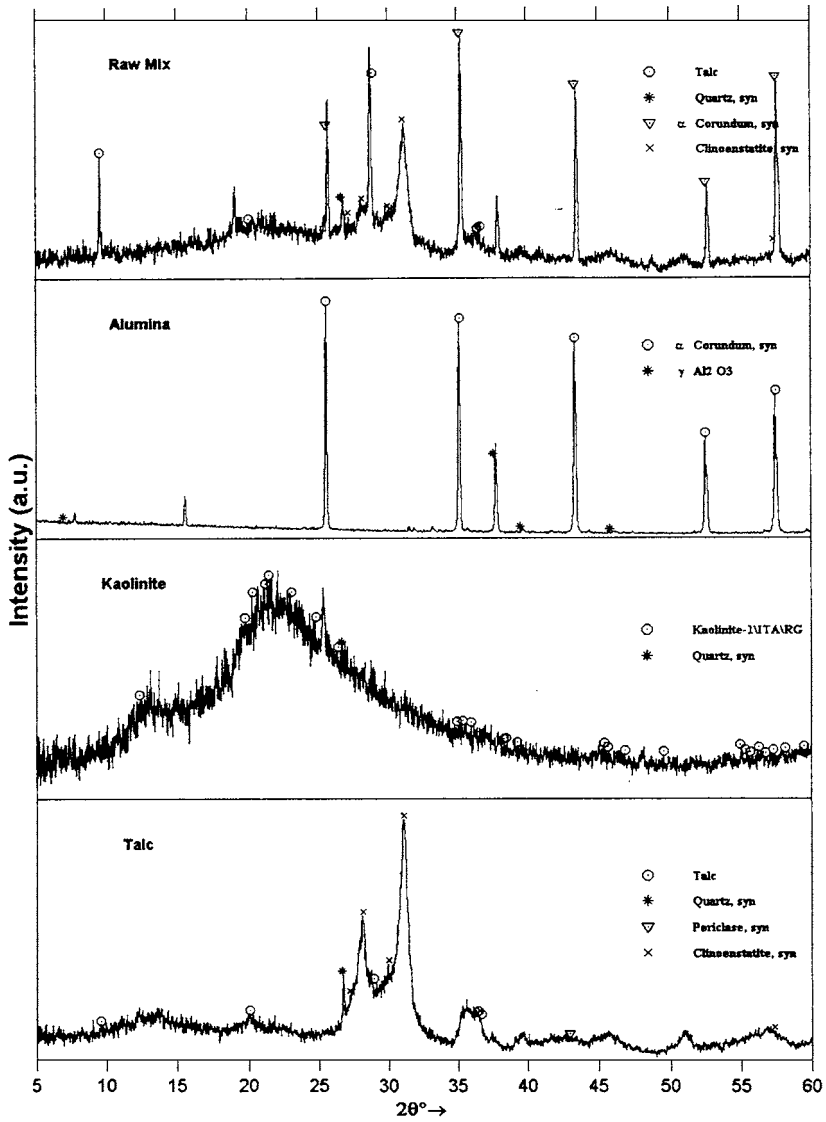

Figure 3 X-ray diffraction patterns of talc, kaolinite, alumina and a honeycomb containing a mixture of talc, kaolinite and alumina in cordierite stoichiometry calcined at 1173 K.

silica to crystobalite overlapped by the initiation of solid state reactions leading to the cordierite formation. Further, a linear shrinkage of 0.12% at 1533 K followed by a linear expansion at 1620 K confirms with the thermal events as observed in TG-DSC curves.

3.3. X-ray diffraction studies

Fig. 3 shows the X-ray diffraction patterns (XRD) of talc, kaolinite and alumina powders calcined for 4 h at 1173 K along with the cordierite raw mix (formulated in the weight ratio 1 : 0.892 : 0.321 of kaolinite, talc and alumina, respectively) and extruded to honeycomb structures. It is evident from Fig. 3 that X-ray diffraction of kaolinite samples at 1173 K shows several amorphous phases with a hump in the region of 15–30° 2θ, along with quartz resulting from the break down of meta-kaolin lattices. Bindley *et al.*, have also reported similar observations like amorphous band at these angular regions, based on their studies [22]. XRD patterns of talc calcined at 1173 K show the presence of quartz, clinoenstatite along with the un-decomposed talc. XRD patterns of alumina showed the presence of α-Al_2O_3 along with the small amounts of γ-Al_2O_3, which is expected. However, the raw mix at 1173 K showed several peaks in addition to the peaks corresponding to individual un-reacted raw materials or their decomposition products indicating the solid state reactions or transformations of their decomposition products.

Fig. 4 shows the XRD patterns of honeycombs calcined at 1373 K, 1523 K, 1623 K, 1693 K, 1703 K and 1713 K for 4 h. From this figure, it is clear that at 1373 K the talc completely changes into clinoenstatite ($MgSiO_3$) form, a high temperature stable form along with the appearance of mullite ($3Al_2O_3{\cdot}2SiO_2$) from metakaolin. Cordierite phase development starts at 1523 K as is evident from the appearance of the characteristic lines at 10.4° 2θ corresponding to the Miller indices (020) and (110).

At 1623 K, cordierite phase ($Mg_2Al_4Si_5O_{18}$) emerges as a major phase with its concentration around 52% at the expense of other phases as compared to the phases observed up to 1523 K. On further heating to 1693 K, the concentration of cordierite phase further increases to more than 90% with the minor phases such as α-Al_2O_3, mullite and spinel. However, on further heating to 1703 K, it was observed that the sample undergo softening followed by melting at 1713 K resulting in the

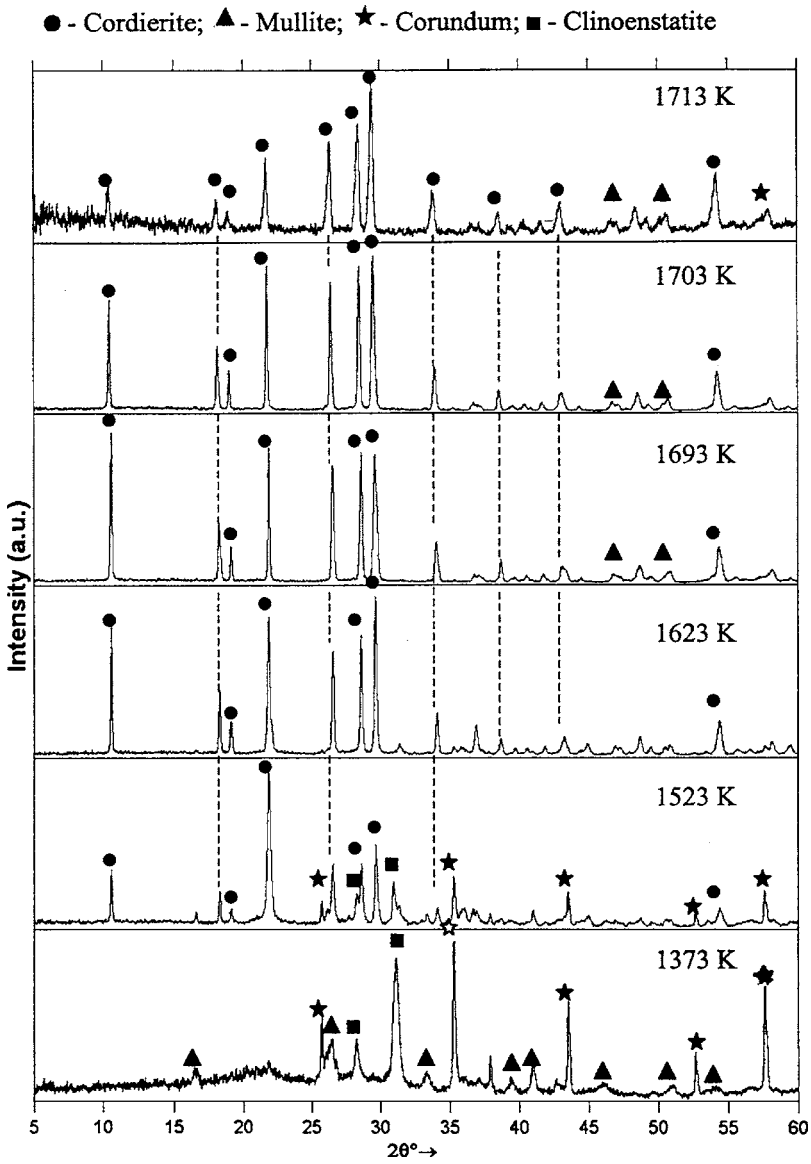

Figure 4 X-ray diffraction patterns of cordierite honeycomb sintered at temperatures between 1173 K and 1713 K.

collapse of the channels along with the corresponding decrease in cordierite phase to 28%. These results are well correlated with the observations made in the earlier studies [6, 13, 23].

3.4. Effect of cordierite content on coefficient of thermal expansion

The bulk density, apparent porosity and water absorption values of sintered cordierite honeycomb are found to be 1.6 g/cc, 27% and 17%, respectively. A plot of cordierite content as obtained from the XRD investigations versus coefficient of thermal expansion values from 303 K to 973 K (after incorporating the calibration correction with fused silica standard) is shown in Fig. 5. It is evident that as the temperature increases from 1653 K to 1673 K the cordierite content was increased from 54% to 72% with corresponding gradual decrease in CTE from 2.86×10^{-6}/K to 1.72×10^{-6}/K. The maximum cordierite content of around 90% at the sintering temperature of 1693 K corresponds to the lowest CTE of 0.74×10^{-6}/K. On increasing the sintering temperature further to 1703 K the cordierite content reduced to 68.6% with corresponding increase in CTE to 1.2×10^{-6}/K. When the sintering temperature was further raised to 1713 K the CTE further increased to 2.4×10^{-6}/K, which might be due to the collapse of the honeycomb structures along with the decrease of cordierite content to 28%. Therefore, the cordierite content along with other phases is playing a dominant role in determining the CTE.

The cordierite generally exhibits a bulk thermal expansion of 1.5×10^{-6}/K in the temperature range of 303 K to 973 K [9]. However, the thermal expansion of 0.74×10^{-6}/K in case of these honeycomb structures can be attributed to the preferred orientation of cordierite crystals, which are highly anisotropic in nature [1]. It is well known that cordierite exhibit a hexagonal ring structure by sharing the corners of five silicon and aluminum tetrahedra with additional tetrahedra and magnesium octahedra network connecting the alternate hexagonal rings [24, 25]. This configuration results in the formation of two structural holes or vacant sites per unit cell parallel to the c-axis of the crystal. This results in a negative expansion along the c-axis and a positive thermal expansion along the other axes. This thermal

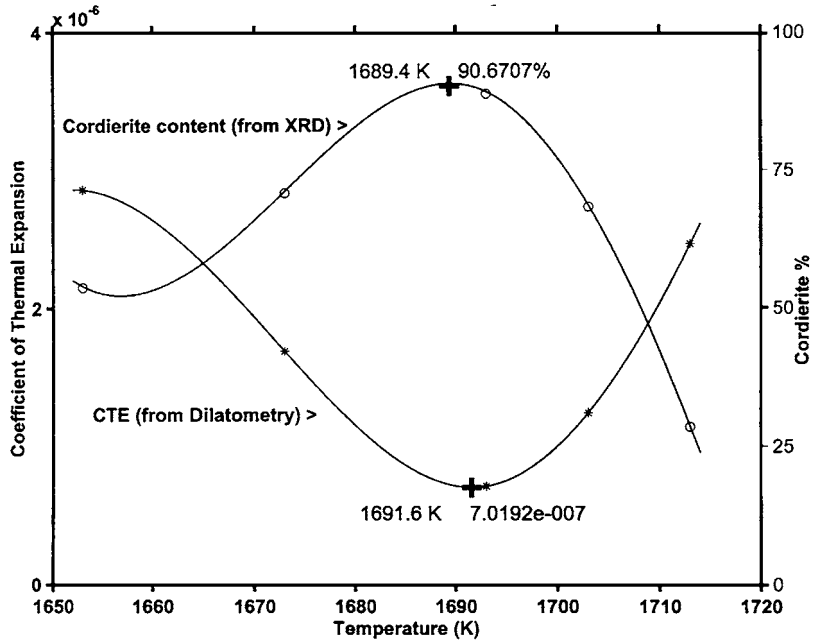

Figure 5 Variation of co-efficient of thermal expansion as a function of cordierite content in the sintered honeycombs.

anisotropy induces thermal stresses in polycrystalline cordierite honeycomb structures, which results in the formation of micro-cracks [26]. In addition, the presence of other phases with higher coefficient of thermal expansion such as α-Al_2O_3 (9×10^{-6}/K), $MgAl_2O_4$ (8.8×10^{-6}/K), $Al_6Si_4O_{13}$ (4.5×10^{-6}/K) in the matrix of low expanding cordierite $Mg_2Al_4Si_5O_{18}$ (1.5×10^{-6}/K) causes thermal strain which induces micro-cracks. The presence of micro-cracks is also evident from the hysteresis of the dilatometric curve (incorporating sample holder correction) recorded while heating (from RT to 973 K) and (from 973 K to RT) for sintered honeycomb samples as depicted in Fig. 6. When the honeycombs are heated, the crack healing occurs and on cooling the internal stresses become large, which reinitiate the microcrack formation leading to hysterisis in thermal expansion [27]. On thermal cycling the cracks open and close thereby compensating the dimensional change which otherwise manifested as the thermal expansion.

Hochella *et al.* [28] attempted to correlate the thermal expansion properties of cordierite with structural changes as a function of increasing temperature. On heating the sample, due to its unique structural features described above and anisotropic expansion of MgO octahedra results in the rotation of six numbered rings in clockwise and anti-clockwise direction in alternate layers perpendicular to c-axis. This interplay of the tetrahedral framework is associated with the change in bond angles contributing towards lower expansion.

3.5. Thermal anisotropy in solid and honeycomb cordierite samples

The CTE values of the cordierite solid rod specimens and the honeycomb (along the channels and across the

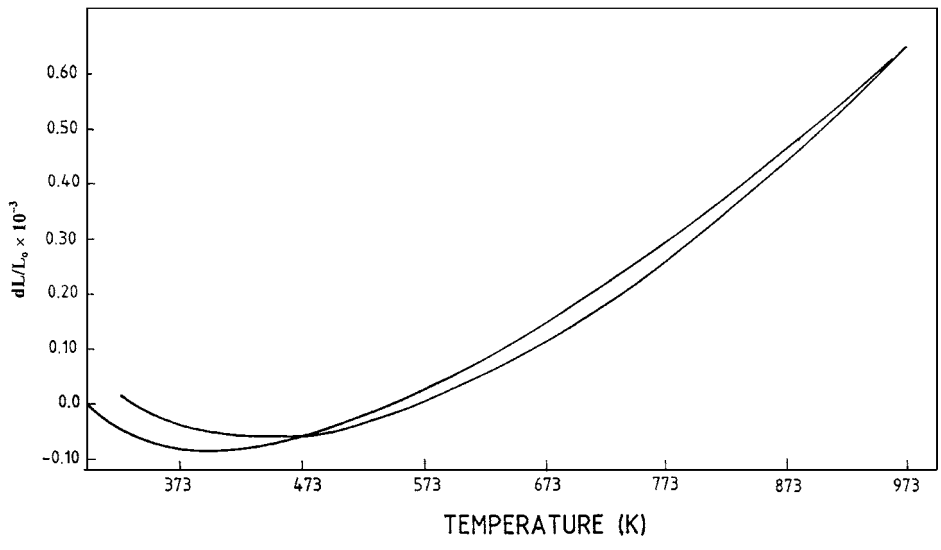

Figure 6 Thermal expansion hysterisis loop of cordierite honeycomb showing the evidence of micro cracking.

TABLE II Transverse I ratios and coefficient of thermal expansion values of honeycombs and solid rods sintered at 1693 K for 4 h

S. No	Specimen identification	Coefficient of thermal expansion ($\times 10^{-6}$/K)	Transverse I ratio
1	Solid Cordierite	1.1	0.56
2	Honeycomb along the channels	0.74	0.30
3	Honeycomb across the channel	1.42	0.70

channels) and the corresponding transverse intensity (I) ratios calculated from the XRD patterns of the solid rod, honeycomb samples along with the CTE values are given in Table II. It is evident from Table II that the solid rod specimens show thermal expansion of 1.1×10^{-6}/K, which is higher in comparison with the value of 0.74×10^{-6}/K observed for honeycomb samples along the direction of extrusion. In addition to this, a higher CTE value of 1.42×10^{-6}/K was observed for honeycombs across the direction of extrusion as compared to that of along the extrusion direction.

Lachman *et al.* [1, 3] have reported that the cordierite samples with preferentially oriented crystals along with C-axis generally exhibit a lower transverse I ratio in comparison to the samples with randomly oriented crystals. Thus, the lower CTE of 0.74×10^{-6}/K and the corresponding low transverse I ratio of 0.30 observed with present study for the honeycomb samples along the direction of extrusion can be attributed to the preferential orientation of cordierite crystals along the C-axis in the direction of extrusion. This is further evident from the transverse I-ratio of 0.56 observed for the solid rod along the direction of extrusion and the crystal transverse I-ratio of 0.70 observed across the direction of extrusion in the case of honeycombs, in which the orientation of cordierite crystals are considered to be random. The preferred orientation in case of honeycombs can be attributed to the higher degree of shear stresses being imposed on the dough during the honeycomb extrusion process and also due to the sintering schedule adopted. The preferred orientation of cordierite crystals leads to the different CTEs along and across the direction of extrusion of honeycomb leading to thermal anisotropy. Thus, these results are well correlated with the observation made by Lachman *et al.* [1, 3].

3.6. Effect of CaO on CTE of honeycombs

Cordierite honeycombs doped with 0.5%, 1.0% and 1.5% of CaO were sintered at 1673 K for 4 h and were subjected to dilatometric measurements (using fused silica as a calibration standard) from 303 K and 973 K and also by X-ray diffraction studies. A marginal increase in bulk density to 1.65 g/cc and corresponding decrease in apparent porosity to 25% and water absorption to 15% was observed in comparison to the un-doped cordierite honeycomb samples when it was doped with 1.5 mass % CaO. The CTE values are plotted in Fig. 7A as a function of CaO content. It can be seen from Fig. 7A that a lowest CTE value (0.74×10^{-6}/K) for honeycomb doped with 0% CaO, however,

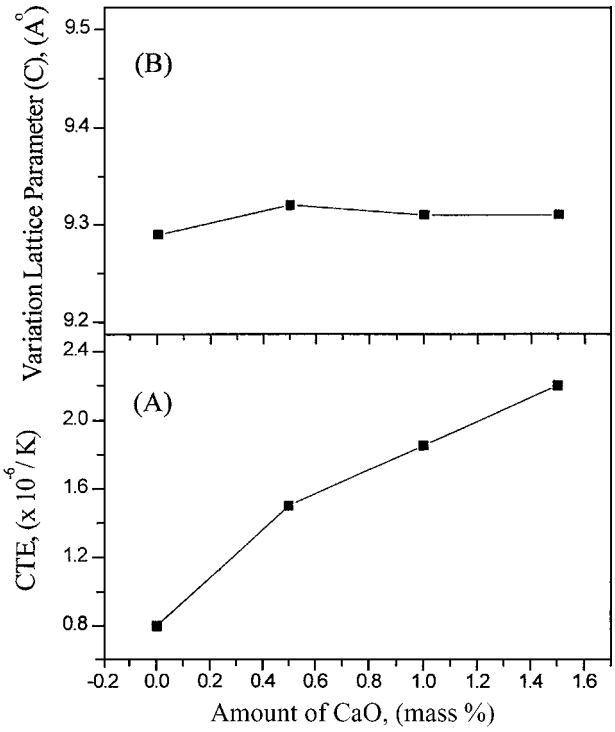

Figure 7 Effect of CaO content on (A)-CTE and (B)-c-axis lattice parameter of cordierite honeycomb sintered at 1673 K for 4 h.

with the increase of CaO content to 1.5%, the CTE value increased to 2.23×10^{-6}/K. This clearly indicates the major role of CaO in determining the CTE. Lachman *et al.* [3] have also reported an increase of CTE with the increase of CaO restricting the preferential orientation of cordierite crystals in the honeycomb structures [3, 25] by influencing reactions and thermal events during the firing cycle.

In order to see the effect of CaO doping on cordierite lattice, the precision lattice parameters were calculated from the experimental XRD data, using NBS*83 computer evaluation program obtained from International Centre for Diffraction Data (ICDD), USA. A plot showing the effect of c-parameter as a function of CaO content are given in Fig. 7B. It is evident from Fig. 7B that there is an increase in c-lattice parameter with respect to CaO content may be due to the presence of doped Ca^{2+} atoms occupying the vacancies parallel to the c-axis formed by the layered cordierite structure as described above.

Thus, as the temperature increases, the Ca^{2+} occupying the vacancies may inhibit the contraction along the c-axis and hence the thermal expansion compensation may not occur for other axes leading to low anisotropy [29]. This results in high thermal expansion values. In addition to this, considering the Mg^{2+} site the bulk thermal expansion is not only dependent on the expansion of Mg–O bonds but also on the size consideration of the atom occupying the Mg^{2+}-site. Ca^{2+} with high ionic radii in comparison to Mg^{2+} partially occupying the octahedral site may also hinder the clockwise and anti-clock wise rotation of octahedral rings leading to higher expansion values.

A typical dilatometric curve recorded (incorporating sample holder correction) for the calcium doped cordierite from (RT to 973 K) and from (973 K to RT)

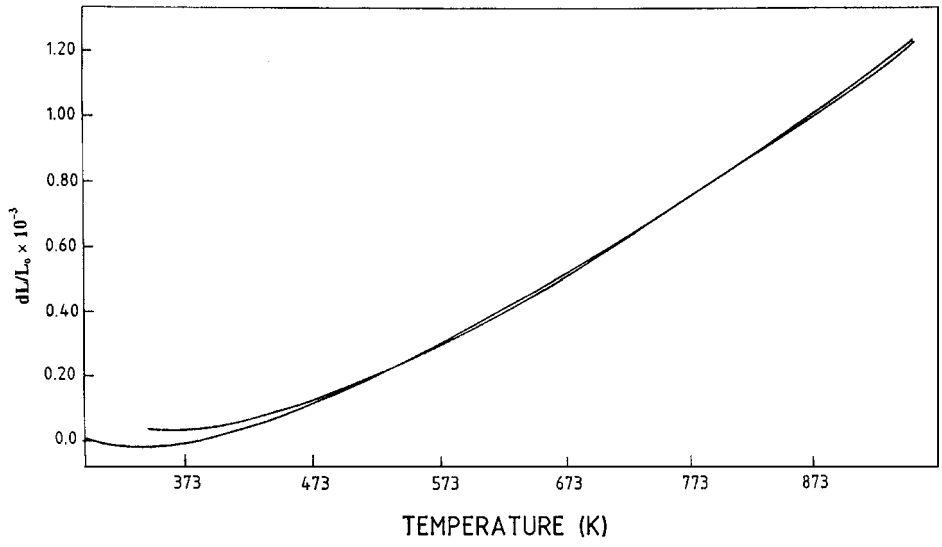

Figure 8 Thermal expansion hysterisis loop of cordierite honeycomb doped with 1.5 mass% CaO.

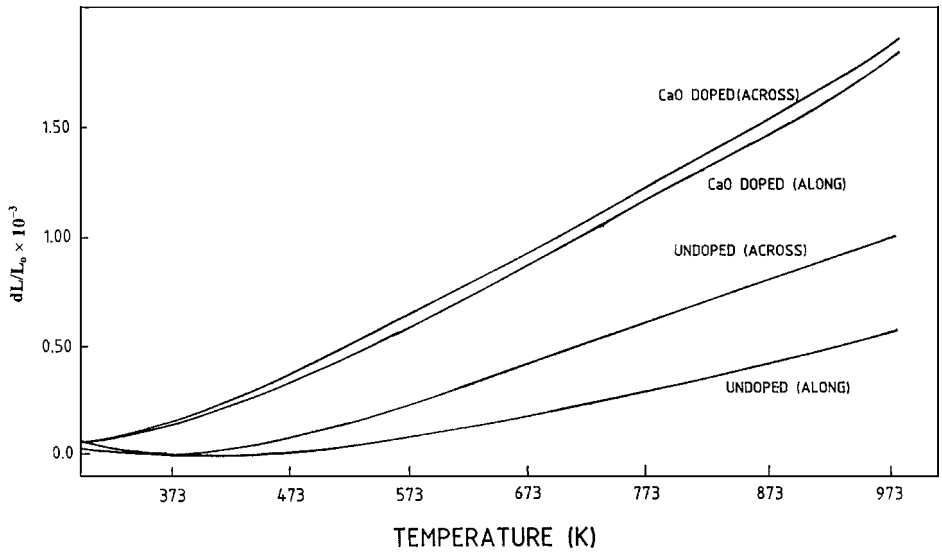

Figure 9 Thermal expansion curves of honeycombs without doping and doped with 1.5 mass% CaO recorded along and across the channels.

is shown in Fig. 8. This curve clearly shows a low thermal hysteresis in comparison with the un-doped honeycomb sample indicating significant reduction in the amount of micro-cracks. This can be correlated with the low anisotropy in axial thermal expansion induced because of the calcium doping to the cordierite crystallites as described above. Moreover, the increase in thermal expansion values observed for the calcium-doped honeycombs can be attributed to the decrease in the thermal anisotropy further leading to a decrease in the amount of microcracks with the increase of Ca^{2+} content. The thermal expansion curve of the honeycomb recorded (along and across the direction of extrusion) for undoped honeycomb and honeycomb doped with 1.5% CaO from room temperature to 973 K is shown in Fig. 9. It is evident that though there is an overall increase in the CTE due to the doping of Ca^{2+}, a significant reduction in anisotropy can be achieved for honeycomb structure by doping with Ca^{2+}. These observations can be well correlated with the earlier studies [29].

4. Conclusions

1. The honeycomb structure extruded from indigenously available precursor oxides such as kaolinite, talc and alumina was subjected to TG-DSC, dilatometry and XRD investigations. The evolution of cordierite through a series of transformations or solid state reactions of these precursor oxides at various processing temperatures has been identified.

2. A maximum cordierite content of greater than 90% and a corresponding lowest CTE of 0.74×10^{-6}/K has been observed at 1693 K soaked for 4 h with respect to the indigenous raw materials and processing conditions employed in the present study. The honeycomb samples exposed to more than 1693 K resulted in the decomposition of cordierite leading to relatively high coefficients of thermal expansion.

3. Honeycomb samples sintered have shown a low CTE (RT-973 K) of 0.74×10^{-6}/K along the direction of extrusion and 1.42×10^{-6}/K across the direction of extrusion in comparison to the solid rod samples exhibited a CTE of 1.1×10^{-6}/K. These observations

are found to be well correlated with the orientation of cordierite crystallites as revealed from the transverse I ratio calculated from the XRD patterns.

4. The presence of micro-cracks due to the axial anisotropy of the cordierite crystallites and hence low bulk thermal expansion observed are evident from the thermal expansion hysteresis, recorded while heating and cooling cycle of the honeycomb structures.

5. On doping of Ca^{2+}, it is found to occupy the vacancies parallel to the c-axis resulting in corresponding increase in c-lattice parameter, which in turn restricts the contraction along the c-axis leading to a significant reduction in anisotropy. While in thermal cycling, however, an increase in bulk thermal expansion was observed due to the absence of micro-cracks resulting from low anisotropy as revealed by the low thermal hysteresis.

Acknowledgements

The authors are grateful to Dr. G. Sundararajan, Director of this institute for the discussions and for granting permission to publish these results. We also thank Mr. K. Rajasheker Reddy, Mr. K.V. Ramana, and Mr. Shaik Ahmed for their technical assistance.

References

1. I. M. LACHMAN and R. M. LEWIS, U.S. Patent No. 3,885,977, May 27, 1975.
2. T. HARADA, T. HAMANKA, K. HAMAGUCHI and S. ASAMI, U.S. Patent No. 4,869,944, Sep. 26, 1989.
3. I. M. LACHMAN, R. D. BAGLEY and R. M. LEWIS, *Bull. Am. Cerm. Soc*. **60**(2) (1981) 202.
4. P. M. THEN and P. DAY, *Interceram* **69**(1) (2000) 20.
5. H. KAINER and H. REH, *ibid.* **40** (2) (1991) 99.
6. R. JOHNSON, B. P. SAHA, I. GANESH, V. MAHENDER, S. BHATTACHARJEE, Y. R. MAHAJAN and M. M. K. KHAJA, *Trans. Indian. Ceram. Soc.* **59**(3) (2000) 93.
7. T. M. GARDNER, S. E. LOTT, S. J. LOCKWOOD and L. I. MCLAUGHLIN, U.S. Patent No. 5,830,421, Nov. 3, 1998.
8. H. RAY, *Interceram* **5** (1987) 54.
9. J. P. DAY and D. L. HICKMAN, *J. Am. Ceram. Soc.* **52** (1995).
10. Y. R. MAHAJAN and R. JOHNSON, in " Materials Research: Current Scenario and Future Projections," edited by R. Chidabaram (Materias Reseach Society of India, 2003) (in press).
11. P. GROJEAN, *Interceram* **42**(1) (1993) 86.
12. U. SELVARAJ, S. KOMARNENI and RUSTUM ROY, *J. Am. Cerm. Soc.* **73** (12) (1990) 3663.
13. M.-A. EINARSRUD, S. PEDERSEN, E. LARSEN and T. GRANDE, *J. European Ceram. Soc*. 19 (1999) 389.
14. H. G. WANG, G. S. FISCHMAN and H. HERMAN, *J. Mater. Sci.* **24** (1989) 811.
15. H. M. JANG, *J. Am. Ceram. Soc.* **78**(3) (1995) 723.
16. B. P. SAHA, R. JOHNSON, I. GANESH, G. V. N. RAO and Y. R. MAHAJAN, *Mater. Chem. Phys.* **67**(1–3) (2001) 140.
17. R. JOHNSON, V. JAIN. S. V. KAMAT, I. GANESH, B. P. SAHA and Y. R. MAHAJAN, *J. Advan. Mater.* (in press, 2002).
18. J. HOWITT, in "Catalysis and Automobile Emission Control," edited by A. Crucq and Frennet (Elsavier Science and Publisher).
19. R. MORRELL, *Proc. Brit. Ceram. Soc.* **28** (1979) 52.
20. W. KOTANI, Y. ONO and K. KUMAZAWA, U.S. Patent No. 5,567,663, Oct., 22, 1996.
21. N. SARKAR and G. K GREMINGER JR., *Ceramic Bullatin* **11** (1983) 62.
22. G.W. BRINDLEY and M. NAKAHIRA, *J. Am. Ceram. Soc.* **42**(7) (1959) 311.
23. J. R. GONZALEZ-VELASCO, M. A. G. ORTIZ, R. FERRET, A. ARANZABAL and J. A. BOTAS, *J. Mater. Sci.* **34** (1999) 1999.
24. D. K. AGARWAL, V. S. STUBICAN and Y. MEHROTRA, *J. Am. Ceram. Soc,* **69** (1986) 847.
25. E. P. MEAGHER and G. V GIBBS, *Canadian Mineralogist* **15** (1977) 43.
26. W. P. BUESSEM and F. F. LARGE, *Interceram* **15**(3) (1966) 43.
27. F. A. COSTA OLIVERIA and J. C. FERNANDES, *Ceram. Intern.* **28** (2002) 79.
28. M. F. HOCHELLA JR. and G. E. BROWN, *J. Am. Ceram. Soc.* **69** (1982) 1.
29. S. SUNDER, V. S. S. VEPA and A. M. UMARJI, *ibid.* **76**(7) (1993) 1873.

Received 16 April 2002
and accepted 3 April 2003